Climatic Change (2020) 162:2139–2155
https://doi.org/10.1007/s10584-020-02742-1

A simple grid-based framework for simulating forest structural trajectories linked to transient forest management scenarios in Fennoscandia

Titta Majasalmi[1,2] · Micky Allen[1] · Clara Antón-Fernández[1] · Rasmus Astrup[1] · Ryan M. Bright[1]

Received: 25 September 2019 / Accepted: 14 May 2020/ Published online: 16 June 2020

Abstract

Forest structural properties largely govern surface fluxes of moisture, energy, and momentum that strongly affect regional climate and hydrology. Forest structural properties are greatly shaped by forest management activities, especially in the Fennoscandia (Norway, Sweden, and Finland). Insight into transient developments in forest structure in response to management intervention is therefore essential to understanding the role of forest management in mitigating regional climate change. The aim of this study is to present a simple grid-based framework – the Fennoscandic Forest State Simulator (F2S2) – for predicting time-dependent forest structural trajectories in a manner compatible with land models employed in offline or asynchronously coupled climate and hydrological research. F2S2 enables the prescription of future regional forest structure as a function of: i) exogenously defined scenarios of forest harvest intensity; ii) forest management intensity; iii) climate forcing. We demonstrate its application when applied as a stand-alone tool for forecasting three alternative future forest states in Norway that differ with respect to background climate forcing, forest harvest intensity (linked to two Shared Socio-economic Pathways (SSPs)), and forest management intensity. F2S2 captures impacts of climate forcing and forest management on general trends in forest structural development over time, and while climate is the main driver of longer-term forest structural dynamics, the role of harvests and other management-driven effects cannot be overlooked. To our knowledge this is the first paper presenting a method to map forest structure in space and time in a way that is compatible with land surface or hydrological models employing sub-grid tiling.

Electronic supplementary material The online version of this article (https://doi.org/10.1007/s10584-020-02742-1) contains supplementary material, which is available to authorized users.

✉ Titta Majasalmi
titta.majasalmi@aalto.fi

[1] Norwegian Institute of Bioeconomy Research (NIBIO), Box 115, 1431 Ås, Norway

[2] Aalto University, School of Engineering, Department of Built Environment, Box 14100, 00076 Espoo, Finland

Keywords Climate change · Forest management · Land management · Climate modeling · Forest dynamics · Hydrological modeling

1 Introduction

The heightened role of forest management to mitigate regional climate change necessitates a deeper understanding of how forest harvest and management affects regional surface energy and hydrological budgets through modifications to forest composition and structure. This is particularly true in forest-rich regions like Fennoscandia (Norway, Sweden, and Finland) where most forests are secondary and in a state of transiency (FAO 2019). Insight into the future state of regional forest structure is needed to robustly quantify the 21st century regional climate impact that is attributable to past and future forest management decisions.

Many land model components of climate models dynamically simulate interannual trajectories of forest structure following disturbance. Most land models are area- or grid-cell based, where disturbances are implemented at the level of the grid-cell. In recent years, various approaches have been developed allowing disturbances to be implemented at the sub-grid-cell level, permitting a more detailed accounting of within-forest differences in forest structure, and hence improved modeling of successional dynamics in managed forest environments. This is typically done by increasing the number of sub-grid components in the model. For example, Shevliakova et al. (2009) used the model LM3 that included twelve possible land tiles for all plant functional types (PFTs), employing similarity-based merging to constrain the actual number of tiles. Yue et al. (2018) presented six tiles per PFT, with tile-merging taking place after exceeding pre-defined biomass boundaries. In ORCHIDEE-CAN, three tiles per PFT have been used, with tile merging following the exceedance of predefined diameter thresholds (Naudts et al. 2015). The drawback of such approaches is that the sub-grid information is lost as soon as tile units are merged, which must be done to constrain the number of age or structural classes to save computation costs. To overcome information loss, some have developed separate forest management "modules" to track sub-grid forest structural information outside of the land model (e.g. Organizing Carbon and Hydrology in Dynamic EcosystEms (ORCHIDEE) FMM by Bellassen et al. (2010) and Community Atmosphere Biosphere Land Exchange (CABLE) by Haverd et al. (2018)).

The advancements described above were motivated by the need to improve the representation of forest management actions within the dynamic global vegetation modeling (DGVM) framework. In regional climate and hydrological modeling, however, a DGVM is not required, and computational constraints limiting the number of sub-grid tiles or necessitating tile merging are of less concern. Further, the need to internally resolve trajectories in biomass accumulation (and hence carbon stocks) is non-existent in regional modeling contexts where the research foci are on biogeophysically driven impacts (i.e. those mediated by perturbations to surface energy and moisture fluxes). As such, there appears to be room for the soft-coupling of simplified forest dynamic modeling frameworks to land models in ways that allow the prescription and tracking of sub-grid forest structures through time. Such frameworks do not necessarily need to be process-driven, opening-up the possibility to utilize empirical models calibrated on local observational data – such as that derived from national forest inventories (NFIs).

The aim of this study is to present a simple grid-based framework – the Fennoscandic Forest State Simulator (F2S2) – that can be applied to update surface data in land models

employed in regional climate or hydrological research in Fennoscandia (Norway, Sweden, and Finland). F2S2 builds off of the classification scheme of Majasalmi et al. (2018) which characterizes between- and within-species variation in aboveground forest structure. For each forest class, F2S2 estimates a residence time as a function of user-defined forest management (regeneration) intensity and the local climate. The latter may stem from an independent source or from a regional climate model whose underlying land model is asynchronously coupled to F2S2. In addition to the class-dependent models predicting residence times, F2S2 comprises a method for initializing class disturbance legacies, a set of rules governing class transitions, and a method for prescribing final harvests on the landscape.

In Section 2 we describe the workflow underlying the development of F2S2, including the simulating of long-term stand-level development and fitting of simplified forest dynamic models for estimating class residence times, methods for initializing class disturbance legacies, rules governing class transitions, and the spatial allocation of harvests. In Section 3, we demonstrate F2S2's application by simulating future forest states in Norway as a function of two climate forcing scenarios (i.e. Representative Concentration Pathways (RCPs)) and two harvest intensity scenarios linked to two Shared Socio-economic Pathways (SSPs), and further evaluate the relative importance of model and climate on future forests dynamics. In Section 4 we discuss the merits and limitations of F2S2.

2 Materials and methods

2.1 Simple forest dynamics model development

F2S2 comprises a set of class-dependent simple forest dynamic (SFD) models and methods governing their application. SFD models in F2S2 were developed to add the temporal dimension to the Fennoscandic forest classification scheme of Majasalmi et al. (2018) – henceforth "M18". Briefly, the hybrid forest cover-structure classification of M18 was developed using a four-dimensional k-means clustering of regional forest inventory data. The four dimensions were maximum leaf area index (LAI, m^2/m^2), Lorey's height (m), tree crown length (m), and volume density (m^3/ha). Three main tree species groups (spruce, pine, and deciduous) and four forest development classes (1 to 4, 4 being a developed forest characterized by high leaf area, high Lorey's height, and high volume density) comprise a total of twelve forest classes, and a corresponding Look-Up Table (LUT) provides the median structural properties for each forest class. Multi-source National Forest Inventory (MS-NFI) data from 2015 was used to re-map forest cover in the European Space Agency's CCI Land Cover product (Poulter et al. 2015) into the M18 classification at 0.0028° × 0.0028° (i.e. ~300 m) spatial resolution. The fractional area of the twelve forest classes within the M18 product grid-cells are preserved (i.e., termed "percentage layers" in M18 which is analogous to sub-grid tiles used in LSM. For clarity, later on we use 'fractional area' of forest class to refer these data). The non-forest grid-cells are taken from CCI LC-product, and assumed here invariant.

The SFD workflow is described succinctly as follows. For each forest class of each M18 grid-cell we estimate the residence time as a function of local climate (described in Section 2.1.2). The residence time is the number of years that will take a fractional area of a M18 grid-cell to move to the next class (e.g. from class spruce 1 to class spruce 2). The residence time can vary at each time step, since local climate can change at any time step. To estimate when the fractional area of each M18 grid-cell will move to the next class, the relative

developmental stage (RDS) is calculated for each class within the M18 grid-cell at each time step. The RDS is defined as a value from 0 to 1 that indicates how far the class is from the next class (0 being the farthest and 1 being the closest). The RDS is calculated at each time step (t) for each class (n) of each species (i) and M18 grid cell (j) as:

$$RDS_{t,n,i,j} = RDS_{(t-1),n,i,j} + L/RT_{t,n,i,j} \quad (1)$$

Where L is the simulation period length (e.g. 5 years) and RT is the residence time at time step *t* calculated with Eq. 2 (described in Section 2.1.2). When RDS_{ij} reaches 1, the pixel will move to the next class.

We used results from forest growth simulations to fit models for residence time (the SFD model, see Section 2.1.2) that depend on local climate and management intensity. We used the single tree simulator SiTree (Antón-Fernández and Astrup 2019) to simulate the development in forest structure (starting from a newly clear-cut state) at 5-year time steps over a period of 200 years. The growth functions used in SiTree were fitted to the Norwegian National Forest Inventory (NNFI), and are, thus, representative of the Norwegian forest. We simulated all plots of the NNFI from bare land (no initial trees) for 200 years and classified every NNFI plot at each time step according to M18. Two simulations were carried out applying two sets of management rules governing stand regeneration to describe variation in the intensity of forest regeneration practices (Section 2.1.1).

2.1.1 Long-term stand development simulations with SiTree

We simulated the development of all plots in the latest Norwegian NFI (2013-2017) using the open source single tree simulator SiTree (Antón-Fernández and Astrup 2019). All plots were empty at the beginning of the simulations, and growth and recruitment were simulated according to main species (i.e. spruce, pine or deciduous) productivity and management intensity following rules governing regeneration (i.e. establishment + planting), recruitment, and mortality. Simulations were carried out for two rule sets describing a business-as-usual (BAU) and more intensive (H) level of management (Table 1). No harvests (e.g. no thinning or final felling) were implemented over the simulations, and growth, mortality and ingrowth were imputed using data from the last three full NFI inventories. Management intensity scenarios were classified as either BAU or H (essential difference being the planting density

Table 1 Number of trees per hectare used to initiate stands in forecasting National Forest Inventory (NFI) plots by species and management intensity: H= 'high' management intensity and BAU= business-as-usual management intensity. Note, for deciduous species only one management option was used

Species	Management	Number of trees per hectare	
		Productive	Unproductive
Spruce	H	2000-3000	1000
	BAU	1200-1800	1000
Pine	H	1800-2200	1000
	BAU	1200-1500	1000
Deciduous		1000-2000	1000

after clear-cut harvest, see Table 1) except deciduous forest, which has only one management category (i.e. deciduous broadleaved forests are not considered a commercial species in Norway). Both productive and unproductive forests were included in all management scenarios.

2.1.2 SFD model development

Results from both BAU and H stand-level simulations formed the basis of the SFD model development. Regression equations were fit to predict residence times (RT) of a given species in development classes 1-3 (i.e. c1, c2, or c3) of the M18 classification. The equation form was chosen to allow flexibility to simulate different climate change scenarios by including different climatic variables. For our domain, where growth is limited more by temperature than by precipitation, the final model form (i.e. regression equation) included a parameter to modify the mean RT as a function of mean growing season near-surface air temperature. The equation has the form:

$$RT_{i,n,j} = \beta 0_{RT_{i,n}} + \beta 1_{RT_{i,n}} \left(T_{i,n,j} - \overline{T} \right) \quad (2)$$

where i is the species (spruce, pine or deciduous), n is the class number (i.e. c1, c2, or c3), j is the NFI plot, $T_{i,n,j}$ is the plot specific or local mean growing season air temperature (mean of months May – September), and $\overline{T}$ is the mean growing season air temperature over all NFI plots. The intercept parameter, $\beta 0_{RT_{i,n}}$, is defined as the mean RT for a given species and development class (i.e. c1, c2, or c3) at the mean growing season temperature $\overline{T}$. In this exercise, we decided to use growing season (i.e. May-September) monthly mean air temperature, instead of annual temperature, as $\overline{T}$ has a higher correlation with forest productivity (i.e. potential winter-time related artifacts in the data are avoided). The $\overline{T}$ was determined to be 11.2 ^{0}C based on all NFI plot estimates in the fitting data set.

Equation (2) was fitted separately for each management intensity (Table 1), species and forest class, yielding 18 unique sets of parameter estimates. In each independent fit, parameter estimates were obtained using ordinary least squares regression which minimizes the sum of squared differences between the observed and predicted values. In all cases, model fitting was performed within the open source statistical software R (R Core Team 2017). Resulting parameter estimates and fit statistics are presented in Section 3.1.

2.2 Model application

2.2.1 Overview

The SFD models described above can now be applied to update forest state information in a land or hydrological model given user defined harvest volumes and climate. The climate – or in our case, the May-September monthly mean near surface air temperature – can be based on outputs from a climate model simulation performed elsewhere, or, alternatively, from a regional climate model coupled asynchronously to the SFD models run in iteration, as illustrated in Fig. 1.

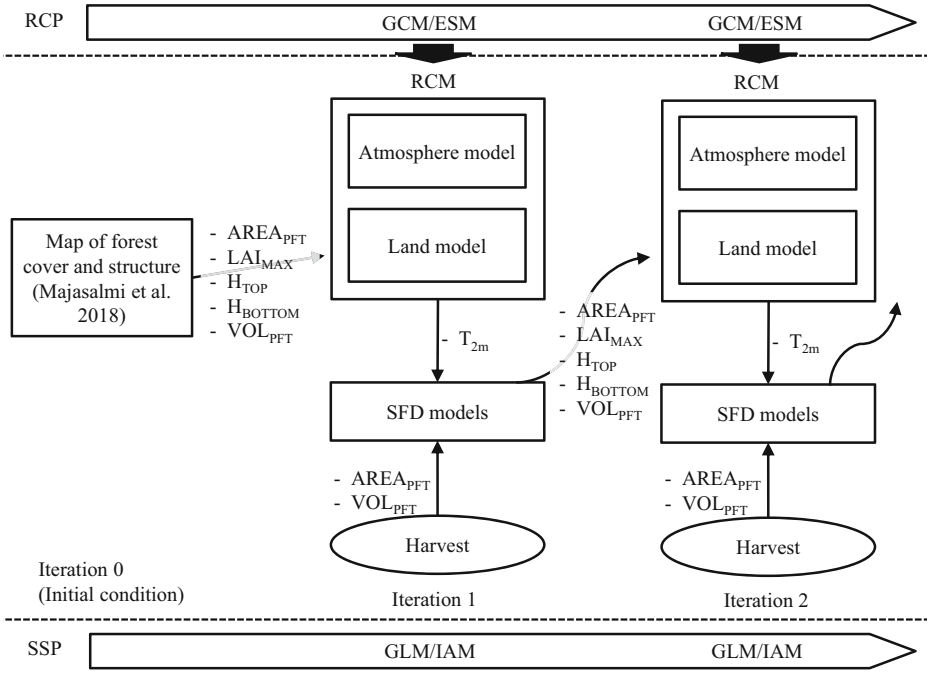

Fig. 1 Schematic illustrating the application F2S2's simple forest dynamic (SFD) models in asynchronously coupled regional climate modeling research. Abbreviations: $AREA_{PFT}$= area dominated by plant functional type (PFT) development class, LAI_{MAX}= Maximum growing season leaf area index, H_{TOP}= tree height, H_{BOTTOM}=canopy height, VOL_{PFT}= stem volume density, GCM= General Circulation Model, ESM= Earth System Model, RCM= Regional Climate Model, GLM= Global Land Model, IAM= Integrated Assessment Model, RCP= Representative Concentration Pathway, SSP= Shared Socio-economic Pathway

2.2.2 Class transitions

In F2S2, classes are only allowed to increase (natural disturbances are implicitly represented in simulations forming the basis of model fitting), and classes remain in the most developed class 4 (i.e. c4) until a harvest is prescribed.

For any given fractional area of a grid-cell of species i at time step t, the class transitions are governed by the relative developmental stage (RDS) (Eq. 1). When RDS reaches 1 the fractional area of the grid-cell will move to the next forest development class unless a harvest is prescribed:

$$n(t) = \begin{cases} n+1 \rightarrow RDS_{t,i,j} \geq 1 \\ n \rightarrow RDS_{t,i,j} < 1 \\ 1 \rightarrow t-1 = harvest \end{cases} \quad (3)$$

where the development class n at time step t increases by one class when RDS equals or exceeds unity, remains unchanged when RDS is less than unity, or equals 1 when a harvest is prescribed in the previous time step.

2.2.3 Initialization

Prior to SFD model application, an initialization procedure was conducted to assign legacies (an initial value RDS, $RDS_{0,n,i,j}$) to the present day ('pd') forest state for classes 1-4 in the M18

product (Note, class 4 remains in class 4 until final harvest). The initialization is done through a random draw that assigns a factor between 0 and 0.99 signifying a distance-to-class transition that occurs at unity (Eq. 3).

2.2.4 Allocation of harvests

Information on the fractional area of the 12 forest classes within the M18 product grid-cells (i.e., termed "percentage layers" in M18; analogous to sub-grid tiles) is used to allocate harvests on the landscape. Harvests are prescribed at the grid-cell level, meaning that all forests within the grid-cell are harvested irrespective of their sub-grid-cell species compositions and class development stages. Given that most final harvests in the study region are carried out by clear-felling, and that harvested stands typically contain a mix of species, this methodological decision mimics the conventional management practice. Harvests are allocated on the landscape in the following manner:

First, pixels are ranked by species based on area-weighted volume density (AWVD, m^3 m^{-2}) computed as:

$$AWVD_{i,s} = \left(\sum_{c=1}^{4}\left(VD_{s,c} \times PL_{i,s,c}\right)\right)/\sum_{s=1}^{3}\sum_{c=1}^{4} PL_{i,s,c} \tag{4}$$

where VD is the volume density (m^3 m^{-2}) from the M18 LUT for species s and class c (four development classes per species) PL is the percentage layer value for pixel i, species s, and class c, and where the term in the denominator represents the total forest area percentage in pixel i. Because total forest area need not necessarily sum to 100% of the grid cell area, weighting by volume density rather than the actual pixel volume reduces bias associated with larger-area grid cells (since we are working with a non-equal area grid).

Following ranking, the top-ranked pixels are selected for harvest (H) until the net total volume harvested approximately equals the target volume (TV; m^3) of the exogenously-defined harvest intensity scenario. This is done in three iterations, starting first with deciduous broadleaf, then pine, then spruce:

$$\begin{aligned}
H^{I} &= \sum_{i=1}^{n} V_{i,Decid.} + \sum_{i=1}^{n} \rho_{i,Pine} + \sum_{i=1}^{n} \rho_{i,Spruce} \rightarrow \sum_{i=1}^{n} V_{i,Decid.} \approx TV_{Decid} \\
H^{II} &= \sum_{i=1}^{n} V_{i,Pine} + \sum_{i=1}^{n} \rho_{i,Decid.} + \sum_{i=1}^{n} \rho_{i,Spruce} \rightarrow \sum_{i=1}^{n} V_{i,Pine} \approx TV_{Pine} - \sum_{i=1}^{n} \rho_{i,Pine}\left(H^{I}\right) \\
H^{III} &= \sum_{i=1}^{n} V_{i,Spruce} + \sum_{i=1}^{n} \rho_{i,Decid.} + \sum_{i=1}^{n} \rho_{i,Pine} \rightarrow \sum_{i=1}^{n} V_{i,Spruce} \approx TV_{Spruce} - \sum_{i=1}^{n} \rho_{i,Spruce}\left(H^{II}\right) - \sum_{i=1}^{n} \rho_{i,Spruce}\left(H^{I}\right)
\end{aligned} \tag{5}$$

where the total volume harvested in the first iteration (H^I) equals the sum of deciduous pixels $i \rightarrow n$ from a sorted list of deciduous pixels ranked by total volume $V_{Decid.}$ which approximately equals the target volume for deciduous (TV_{Decid}) plus the sum of all pine and spruce residuals (i.e., $\rho_{i,\ Spruce}$ and $\rho_{i,\ Pine}$) that is harvested alongside deciduous. In other words, the number of pixels harvested n in the first harvest iteration (H^I) is determined by the number of ranked pixels whose total volume ($\Sigma V_{Decid.}$; m^3) approximately equals the target volume (TV_{Decid}) for deciduous. In the second iteration (H^{II}), the top-ranked pine pixels are harvested until the total pine volume ($\Sigma V_{Pine.}$; m^3) reaches the target volume for pine species, less the total volume of pine residuals harvested in the first iteration. In the third iteration (H^{III}), the top-ranked spruce pixels are harvested until the total spruce volume ($\Sigma V_{Spruce.}$; m^3) reaches the target volume for spruce species, less the total volume of spruce residuals harvested in the first and second iterations.

The total volume harvested in each pixel i for a given species s is computed as:

$$V_{i,s} = \sum_{c=1}^{4} \left(VD_{s,c} \times PL_{i,s,c} \times A_i \right) \quad (6)$$

where A is the total area (m^2) of pixel i.

The rationale for the species ordering (i.e. decid, pine, spruce) of the harvest iterations was to minimize the overharvesting of species with lower target volumes (TV), where for our application region (Norway) $TV_{Decid.} < TV_{Pine} < TV_{Spruce}$. Every single sub-grid unit remains as its own unit across time, which means that they are never merged as they are in e.g. ORCHIDEE (Naudts et al. 2015). In addition, the harvesting routine (Eq. 5) which is applied to the fractional areas of M18 product grid cell ensures that species time-slice specific harvest targets are approximately met in time step except for spruce, for which slight overharvesting may be expected.

2.2.5 Example application in Norway

To illustrate model behavior, we applied our models for whole Norway to simulate 21st century forest dynamics using prescribed harvest volumes linked to two SSPs and prescribed climate forcing linked to two RCPs. RCPs quantify radiative forcing levels relative to pre-industrial values by the end of the 21st century associated with various future greenhouse gas emission scenarios. Near-surface temperature (T_{2m}) corresponding to RCPs 4.5 (moderate mitigation) and 8.5 (no mitigation) are based on bias-corrected multi-model means from EURO-CORDEX (2017) regional climate model simulations downscaled over Norway (Hanssen-Bauer et al. 2009). A 30 m digital elevation model and an environmental lapse rate of 0.65 °C per 100 m were used for the downscaling T_{2m} to a modeling grid matching the Majasalmi et al. (2017) map product (i.e. 0.0028° × 0.0028°). Multi-model means are based on the ten regional climate models: CNRM-CM5_CCLM, CNRM-CM5_SMHI-RCA4, EC-EARTH_CCLM, EC-EARTH_DMI-HIRHAM5, EC-EARTH_KNMI-RACMO, EC-EARTH_SMHI-RCA4, HADGEM2_SMHI-RCA4, IPSL-CM5A_SMHI-RCA4, MPI_CCLM, and MPISMHI-RCA4 for RCP4.5 and RCP8.5. The monthly mean of May-September (i.e. 'growing season') T_{2m} (°C) for the ensemble mean RCP4.5 and RCP8.5 scenarios were averaged for 5-yr time-slices. The present-day ('pd') climate is represented using the ensemble mean RCP4.5 scenarios for the 2016-2020 period.

Species-dependent harvest scenarios for Norway were obtained by statistical downscaling of demographic themes underlying global SSPs (Hu et al. 2018). The SSP framework enables production of hypothetical scenarios that results from combined effects of climate projections, socioeconomic state and political decisions, and facilitates assessments of climate change mitigation and adaptation actions. We used SSP1 'taking the green road', and SSP5 'Fossil-fueled development – taking the highway' which can be combined with RCP 4.5 and 8.5 scenarios. These two scenarios were selected because they present extremes in terms of socio-economic challenges for mitigation ('sustainability' *versus* 'highway') while sharing the same adaptation challenges, and as aforementioned scenario combinations allow linking to Special Report Emission Scenarios (SRES) scenarios B1 (scenario 1) and A1F1 (scenario 2) (Van Vuuren and Carter 2014). As stem volume estimates provide by Hu are underbark (instead of overbark) estimates, the volumes were multiplied with a correction factor (1.15 for conifers and 1.18 for deciduous), before the time-slice specific harvest targets were calculated (Fig. 2). In SSP1 scenario harvest demand will increase >35 mill. m^3, and in SSP5 harvest scenario >73

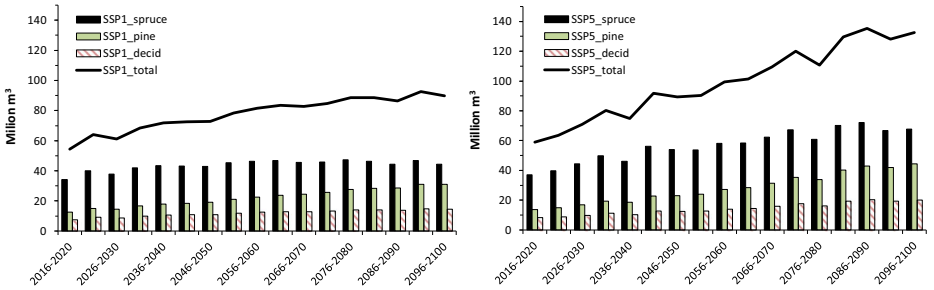

Fig. 2 Time-slice specific harvest targets for spruce, pine and deciduous species following two Shared Socio-economic Pathways (i.e. SSP1 and SSP5). For the present-day ('pd') harvest demand scenario, estimates for 2015 were used

mill. m^3 per 5-yr time-slice. For the present-day ('pd') harvest demand scenario, the harvest demand was set to be 10.1 mill. m^3 per year (i.e. 50.5 mill. m^3 per time-slice), with fixed species shares (70% spruce, 20% pine, and 10% deciduous species).

Two plausible Norwegian RCP-SSP futures were evaluated and compared to a present-day baseline, and three additional scenarios were created to isolate the effects of climate, harvest and management intensity on forest structural development (Table 2).

To extract the climate effect, a scenario combining a pd climate with SSP5 harvest demand and high management intensity (i.e. 'pd_ssp5_H') was compiled, and climate effect extracted as:

$$climate\ effect = \left(\frac{(\text{'rcp85\_ssp5\_H'} - \text{'pd\_ssp5\_H'})}{\text{rcp85\_ssp5\_H}}\right) \times 100\% \quad (7)$$

To extract the harvest intensity effect, an assemble scenario combination of RCP8.5, SSP1 based harvest demand and high management intensity (i.e. 'rcp85_ssp5_H') was gathered, and harvest effect extracted as:

$$harvest\ effect = \left(\frac{(\text{'rcp85\_ssp5\_H'} - \text{'rcp85\_ssp1\_H'})}{\text{rcp85\_ssp5\_H}}\right) \times 100\% \quad (8)$$

The management effect was extracted using scenario combination with RCP8.5, SSP5 based harvest demand, and assuming BAU management intensity (i.e. 'rcp85_ssp5_BAU'):

Table 2 Alternative plausible future scenarios (type=baseline) and scenario combinations (type=effect) used to extract climate, harvest and forest management effects for Norway. Abbreviations: pd= present-day, RCP= Representative Concentration Pathway, and SSP= Shared Socio-economic Pathway (SSP). Note, for deciduous species only one management option was used.

type	climate	harvest	management	scenario name
baseline	pd	pd	BAU	pd_pd_BAU
plausible future	RCP4.5	SSP1	BAU	rcp45_ssp1_BAU
plausible future	RCP8.5	SSP5	H	rcp85_ssp5_H
effect	pd	SSP5	H	pd_ssp5_H
effect	RCP8.5	SSP5	BAU	rcp85_ssp5_BAU
effect	RCP8.5	SSP1	H	rcp85_ssp1_H

$$management\ effect = \left(\frac{(\text{'rcp85\_ssp5\_H'} - \text{'rcp85\_ssp5\_BAU'})}{\text{'rcp85\_ssp5\_H'}}\right) \times 100\% \quad (9)$$

3 Results

3.1 Simple Forest Dynamics models

All SFD models were found significant with $p < 0.005$ and R^2 values varied between 0.24 and 0.01 with a mean of 0.1 (Table 3). The forest management effect on class residence time depended only on growing season temperatures, the slope and intercept being fit separately for each species and management combination. For example, for spruce c1 has a residence time of 45.21 years if the mean growing season temperature equals $\overline{T}$ (was determined to be 11.2 ^{0}C). For each degree increase in the mean growing season temperature over the mean, the residence time decreases by 7.16 years. For spruce, the difference between H and BAU management scenarios is larger than for pines.

3.2 Plausible future scenarios

At the beginning of the simulation, most of the Norwegian forest areas are dominated by spruce or pine belonging to more-developed class c3 (Fig. 3). Around 2040 these forest areas have moved into most-developed class (c4). For deciduous species, in 2015 most of its area resides in class c2, and the general trend is that the areas dominated by intermediate classes c2 and c3 decrease steadily towards the end of the century as transitions from class c3 into most-developed class c4 proceeds. Noteworthy is that, in the baseline '*pd_pd_BAU*' scenario the area belonging to least-developed deciduous class (c1) decreases steadily towards the end of

Table 3 Simple Forest Dynamics (SFD) model coefficients, model significance (p) and coefficient of determination (R^2). Parameter units are years

Species group	Development class	β0	β1	p-value	R^2
'business-as-usual' management intensity					
Spruce	c1	45.21	-7.16	0.00	0.15
	c2	15.06	-3.28	0.00	0.22
	c3	19.78	-4.25	0.00	0.24
Pine	c1	69.07	-4.36	0.00	0.03
	c2	15.83	-1.69	0.00	0.06
	c3	18.62	-1.53	0.00	0.06
Deciduous	c1	90.24	-1.04	0.00	0.01
	c2	50.07	-2.38	0.00	0.03
	c3	38.70	-2.00	0.00	0.07
'high' management intensity					
Spruce	c1	43.35	-6.97	0.00	0.13
	c2	15.54	-3.30	0.00	0.13
	c3	18.47	-3.62	0.00	0.22
Pine	c1	66.43	-3.98	0.00	0.02
	c2	14.67	-1.24	0.00	0.03
	c3	16.71	-0.82	0.00	0.02

the century, whereas in the two climate change scenarios, the abundance of the least-developed class increases for deciduous species.

For spruce, in all scenarios the area belonging to the most-developed class (c4) increases until around 2040-2050 then decreases throughout the latter half of the century. The abundance of the least-developed spruce class c1 stays either increasing or at the same level at the case of baseline scenario, but begins to decrease in the other two plausible future scenarios (Fig. 3dg). For spruce the abundance of intermediate development classes c2 and c3 remains low but slowly increases towards the end of the century.

For pine, there is a similar trend as for spruce, including a fast transition from class c3 into most-developed class c4. However, unlike in spruce, pine least-developed class c1 continues to

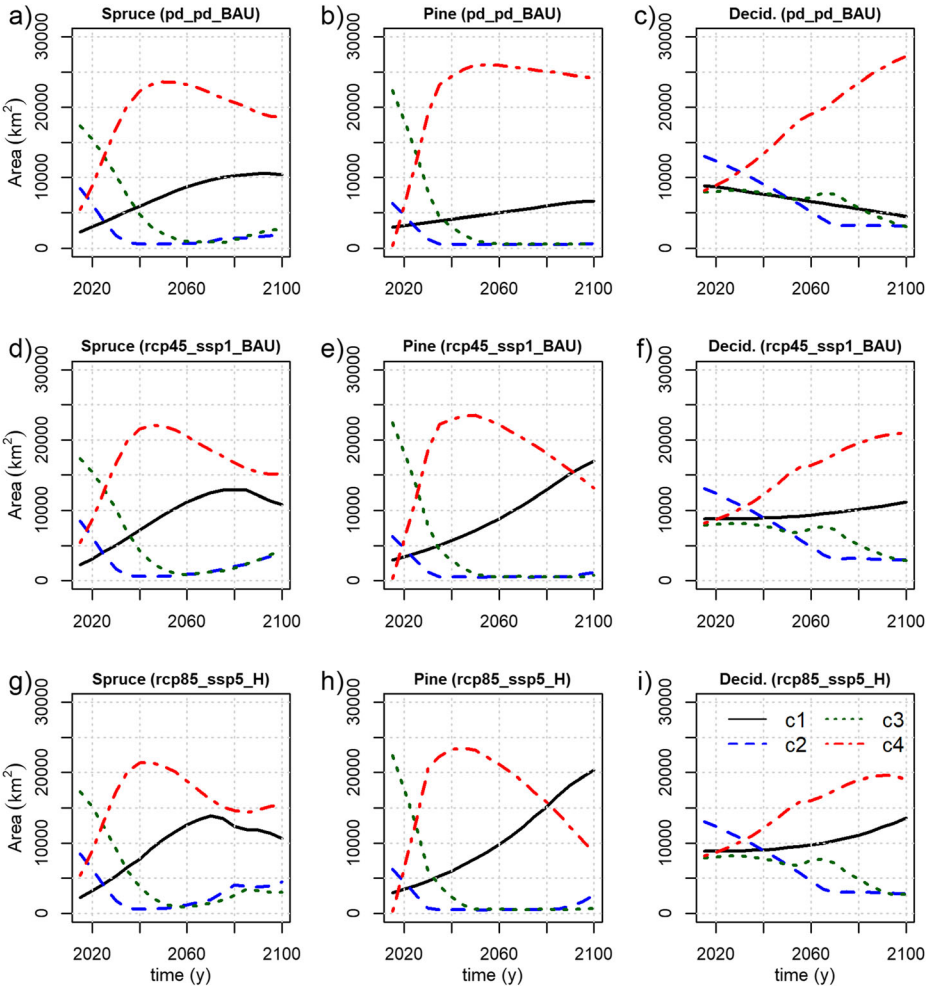

Fig. 3 Simulated development of species classes in Norway following three climate + harvest + management scenarios: **a,b,c)** show baseline scenarios following present-day (pd) climate and harvest intensity and assumes business-as-usual (BAU) forest management intensity i.e. '*pd_pd_BAU*'. **d**, **e**, **f**) show a plausible future scenario following RCP4.5 with SSP1 based harvest demand and assumes BAU forest management intensity i.e. '*rcp45_ssp1_BAU*'. **g**, **h**, **i**) show a plausible future scenario following RCP8.5 with SSP5 based harvest demand and assumes 'high' forest management intensity i.e. '*rcp85_ssp5_H*'

show a positive trend in all scenarios. The abundance of intermediate classes c2 and c3 remains low, similar with spruce.

3.3 Effects scenarios

The isolation and analysis of the effects of climate, harvest and management intensity on the temporal development of forests reveals that climate has the strongest influence on structural development (Fig. 4). The climate effect of increasing temperature is most apparent in spruce dominated areas but less so for areas dominated by pine and deciduous species. Higher harvesting intensity exclusively decreases the area of c4 class across all species.

In spruce dominated areas, warming will result in increases to forest growth indicating faster development class transitions. For spruce, the warming climate may be expected to decrease the relative abundance of the least-developed class c1, and respectively, to increase the relative abundance of most-developed class c4 between 2060 and 2100. Between 2040-2060 class c3's relative abundance will decrease, but as the transition from class c2 to class c3

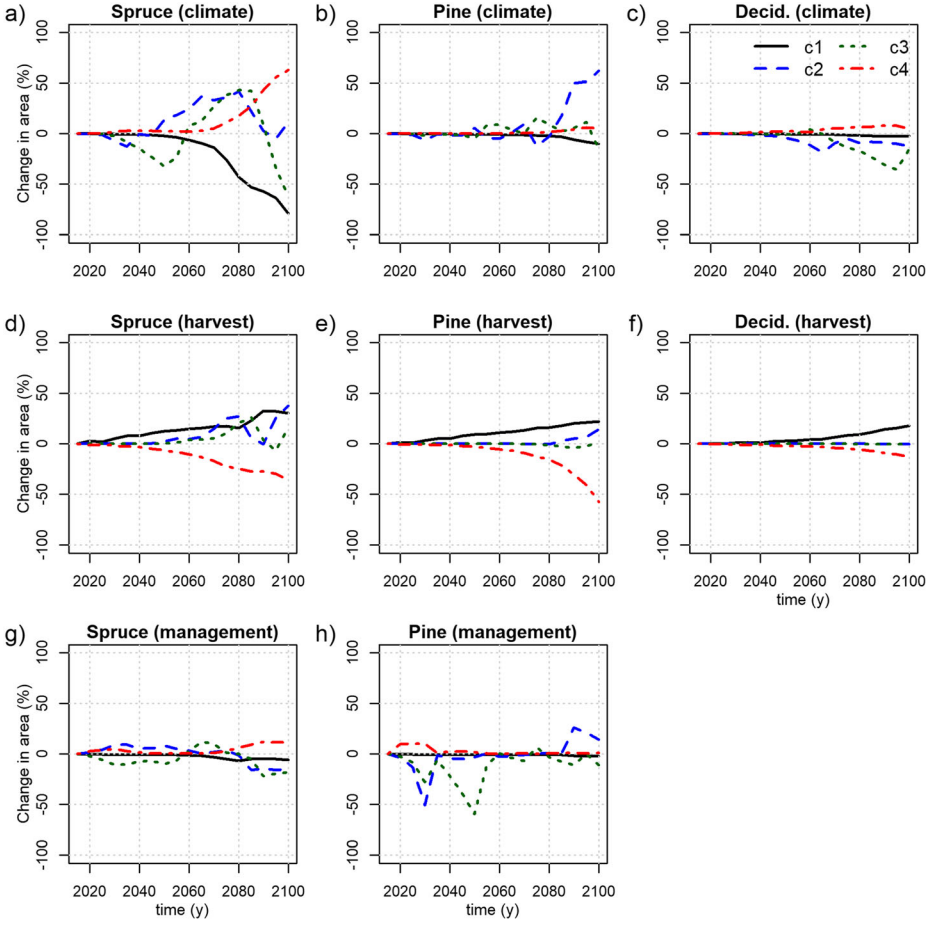

Fig. 4 Attribution of climate, harvest and management intensity effects on structural development class changes. The temporal development of: **a**,**b**,**c**) Climate effects (Eq. 7), **d**,**e**,**f**) harvest effects (Eq. 8) and **g**,**h**) management intensity effects (Eq. 9) on percentage change in abundance of development class areas

increases, the c3 class will become more abundant again. After 2080, c3's relative abundance will sharply decrease due to faster class transitions from c3 to c4.

In pine dominated areas, the climate effect will start to appear only after 2080 (Fig. 4b) where transition speeds from least-developed class c1 to class c2 begin to accelerate, slightly increasing the relative abundance of classes c3 and c4. For deciduous species, the climate warming will slightly increase the relative transition speed from more-developed class c3 to most-developed class c4 during the second half of the century. However, the increasing temperature will be expected to decrease the relative abundance of deciduous intermediate classes c2 and c3.

The harvest effect remains linear for pine and deciduous species but for spruce, some differences between the two SSPs start to emerge around 2065. The larger amount of harvesting in the case of SSP5 than in SSP1 increases the area of least-developed classes. For spruce, the relative abundance of class c2 will start to increase after 2065, followed by relative increase in class c3 ten years later, after which the relative abundance of class c1 will clearly increase. For pine, the increasing harvest amount will decrease most-developed class c4's abundance, with a slight increase in intermediate classes (c2 and c3) relative abundance. For deciduous species the intensity of harvest does not seem to have an appreciable effect on intermediate class c2 and c3 abundances.

The management effect has a larger influence on class transitions in pine dominated areas than in spruce dominated areas (Fig. 4gh). Under high management for pine, the relative abundance of class c2 first decreases (due to transition to c3), and shortly thereafter transitioning from c3 to c4 leads to a decrease in c3 relative abundance. For spruce, the management effect results in smooth temporal transitions on relative class abundances

In both plausible future scenarios, the national mean forest LAI increases only until 2050 whereas in the baseline scenario, the LAI continues to increase until the end of the century (Fig. 5). For *rcp8.5_ssp5_H* the maximum LAI is reached around 2050, whereas for *rcp4.5_ssp1_BAU* the maximum LAI is reached slightly later ~2060. The effect scenarios built around RCP8.5 and SSP5 show that, if RCP8.5 climate is replaced with current climate, the expected decline in LAI is very steep after 2040 (i.e. *rcp8.5_ssp5_H versus pd_ssp5_H*).

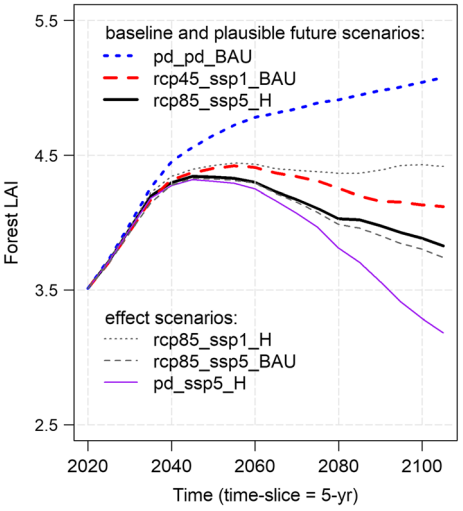

Fig. 5 Simulated development of the mean maximum Leaf Area Index (LAI, m^2/m^2) in Norwegian forests under six scenarios representing different combinations of climate forcing, management intensity, and harvest intensity

Comparing the effect scenarios, if the *rcp85_ssp5_H* harvest rate is reduced to a SSP1-level (‘*rcp85_ssp5_H*’ *versus* ‘*rcp85_ssp1_H*’) the LAI will stay leveled after 2060 until the end of the century. In addition, the results show that the change in management (‘*rcp85_ssp5_H*’ *versus* ‘*rcp85_ssp5_BAU*’) has a small effect on the forest LAI. Noteworthy is that the LAI_{MAX} values fall within the range of measured and modeled values reported for the three boreal tree species (e.g. Majasalmi et al. 2013), and thus all the LAI_{MAX} scenarios are realistic in all scenario combinations.

4 Discussion

In this study, we presented a simple grid-based framework – the Fennoscandic Forest State Simulator – F2S2 – for simulating changes in forest structure in time connected to regional scenarios of future forest management. F2S2 adds the temporal dimension to the hybrid forest cover-structure map product of Majasalmi et al. (2017, 2018) in which forested areas are classified by species and development stage, with each class having a corresponding LUT providing key structural attributes needed to prepare surface data for a land surface or hydrological model. F2S2 comprises a set of simple forest dynamic (SFD) models, calibrated with regional NFI and climate data, along with a set of rules for prescribing final harvests on the landscape and for initializing the current state of transiency in forests (i.e., the accrued residence time since class transition). F2S2 is transparent and flexible, allowing the inclusion of other types of forest management intervention such as tree species change and the implementation of pre-commercial thinning. Tree species change can be implemented by assigning clear-cut harvested pixel areas into other species groups, and pre-commercial thinning can be included by lengthening the residence time of a given class e.g. by zeroing the pixel distance-to-class transition value. In addition, using localized harvest targets, instead of national, might be used to improve spatial allocation of harvests.

The simple growth models presented in this paper model residence time (i.e. growth) as the average residence time for a given class as a function of temperature. Our basic assumption is that temperature is a proxy for site productivity; thus, we assume that productivity increases with higher temperatures therefore giving lower residence times. In Norwegian latitudes, site productivity generally increases with temperature (Antón-Fernández et al. 2016). However other factors, such as soil quality, genetic material of the trees, other climatic factors (e.g. soil moisture, precipitation, frost), and microsite variations are important in explaining variations in site productivity. In forestry, site productivity is traditionally estimated through site index (i.e. the average height of dominant and co-dominant trees within a stand at certain age). Attempts to model site productivity/site index for similar species (Antón-Fernández et al. 2016; Albert and Schmidt 2010) have proved challenging. These site productivity models have R^2 of 0.39-0.56 for Norway spruce, 0.33 for Scots pine, and 0.50 for deciduous species, and include soil quality variables as well as, in some cases, latitude and soil moisture. Thus, it is not surprising that our models, which rely exclusively on temperature as proxy for site productivity, have R^2 that range from 0.15 to 0.24 for spruce, 0.03 to 0.06 for pine, and 0.01 to 0.07 for deciduous species. Given that the variables leading to better growth predictions (like soil quality) are difficult to obtain across large spatial domains (i.e., at climate modeling scales), and often not provided as climate model output (for when F2S2 is asynchronously coupled) - we believe our models represent the best compromise for climate modeling applications that do not simulate forest growth dynamics internally within the land model.

Simulations for Norway in effort to demonstrate F2S2's application and analyze its behavior showed that climate has the largest effect on future forest dynamics, followed by the future harvest demand – both of which were to be expected. The impact of forest management intensity has a lesser, but clear effect on forest structural dynamics. Based on the alternative plausible future scenarios for Norway, the present-day situation dominated by intermediate classes c2 and c3 may be expected to change to the youngest and oldest classes (i.e. c1 and c4) by the synergy of forest dynamics and management actions, which highlights the important role of forest management as a tool for shaping forest structures. Based on the three scenario combinations, one can speculate on two things happening: **i**) the growing stock is reaching its 'maturity'. i.e. forests are aging and further increases in growing stock would require increasing land area occupied by forest (or increasing the number of within PFT development classes to allow finer structural differentiation), and **ii**) larger harvest demand of both SSP scenario combinations results that after 2040 the increasing growth cannot compensate for an increasing demand for forest products. Implications could be to increase area occupied by forests and develop possible strategies to allow more flexibility in species harvest demands (e.g. increase deciduous species harvest).

Comparing predicted future trends in LAI with those of previous works is extremely difficult since few (if any) previous studies have explicitly isolated the effects of climate/environment from forest management on the long-term LAI development in a boreal forest region. We showed the LAI is highly sensitive to both the effects of climate/environment and forest management (i.e. demonstrated in Fig. 5). Although, we suspect that part of the large Climate Modeling Intercomparison Projection (CMIP5) model spread in the predicted future long-term LAI, reported in Mahowald et al. (2016), likely reflects differences in how the underlying land models implement management effects, as much as differences in how LAI is estimated in the model, we nevertheless find that our results generally fall within the ranges reported in Mahowald et al. (2016) for both RCP8.5 and RCP4.5 over all 21st century time slices, and that LAI exhibits a positive relationship with temperature. Noteworthy, is also that not only the selection of RCP scenario influence the projected LAI trajectories, but also the initial mapping of LAI. For example, the recent paper by Majasalmi et al. (2018) (in Figure 6) showed how LAI in Fennoscandia varies spatially within forest PFTs and that ignoring this within-PFT forest structural variation results in almost constant LAI throughout Fennoscandia (Majasalmi et al. 2018). Our framework targets the core of this problem – management impacts on long-term LAI are unknown at present because the models we currently rely on (i.e., CMIP5 models) do not sufficiently account for the effects of management. Due to the importance of LAI for biophysical and biogeochemical interactions, there is ongoing need for improvements for the model mechanisms responsible for the simulations of LAI.

The merits of our framework over those currently applied in climate modeling, are that: **i)** the initial mapping if forest structure is based on high resolution (i.e. pixel resolution of ~ 30 m) MS-NFI data, **ii**) the 0.0028° resolution of our map product allows spatial allocation of forest management actions (e.g. for 61.1° N and 10.5° E in Norway, pixel size of our product is 4.7 ha whereas using 0.5° map products commonly applied in LSMs, the respective pixel size would be 14,939 ha), **iii)** the use of simplified forest dynamics models (SFD), which combine the effects of forest management and temperature, are quick to adapt to new regions and classifications, as they can be calibrated using data simulated from NFI inputs. The main limitation of our framework is that it cannot be used in regions without established NFI inventories due to the need for regional calibration. Thus, we do not expect our framework to be applicable for global modeling studies, as it is developed to fit the needs of regional climate modeling studies allowing

flexible scaling between different spatial resolutions (i.e. using percentage layers or sub-grid areas) to accommodate different exogenously defined climate and harvest data. Although our framework must be soft-coupled to LSMs, we believe it provides more accurate initial mapping than ageless conifer-deciduous classification and generation of trajectories of forest structural development under plausible futures (as a combination of input climate forcing data, and harvest demand and forest management scenarios), which can be directly digested by LSMs.

5 Conclusions

This paper presented a simple modeling framework to capture the general trends in future Fennoscandian forest structure as a function of: climate change, and exogenously defined scenarios of harvest intensity, and forest management intensity. To our knowledge this is the first paper presenting a method to dynamically link forest structural mapping in space and time in a way that is directly applicable to climate modeling studies prescribing land cover transitions. The approach allows regional calibration according to local management practice (i.e. harvest, thinning, management) and climate.

Acknowledgements The research was funded by the Research Council of Norway, grant number 254966/E10 and by Academy of Finland project BOREALITY (grant number 13286390). We thank Stephanie Eisner and Jonathan Rizzi for help with the climate data.

Author contributions TM was responsible for the analysis and had a leading role in writing the paper. RMB, CAF and MA participated in writing the paper. CAF was responsible for SiTree simulations, and MA for SFD model development. All authors participated in conception and design.

Funding Information Open access funding provided by Norwegian Institute of Bioeconomy Research.

Data availability The bias-corrected RCP scenarios were obtained from http://webapp-ext.nve.no/tow/title.aspx?tkey=23192. The enhanced LC-product for Fennoscandia can be loaded from doi.org/10.21350/c9j08bz3.

Compliance with ethical standards

Conflict of interest The authors declare that they have no conflict of interest.

References

Albert M, Schmidt M (2010) Climate-sensitive modelling of site-productivity relationships for Norway spruce (Picea abies (L.) Karst.) and common beech (Fagus sylvatica L.). Forest Ecol Manag 259(4):739–749

Antón-Fernández C, Astrup R (2019) sitree: Single tree simulator. R package version 0.1-6, https://CRAN.R-project.org/package=sitree

Antón-Fernández C, Mola-Yudego B, Dalsgaard L, Astrup R (2016) Climate-sensitive site index models for Norway. Can J For Res 46(6):794–803

Bellassen V, Le Maire G, Dhôte JF, Ciais P, Viovy N (2010) Modelling forest management within a global vegetation model—Part 1: Model structure and general behaviour. Ecol Model 221:2458–2474

EURO-CORDEX (2017) EURO-CORDEX, http://webapp-ext.nve.no/tow/title.aspx?tkey=23192. Downloaded: 17 Feb 2018

FAO (2019) http://www.fao.org/3/X4109E/X4109E05.htm. Accessed: 5 July 2019

Hanssen-Bauer I, Drange H, Førland EJ, Roald LA, Børsheim KY, Hisdal H, ... and Sundby S (2009) Klima i Norge 2100. Bakgrunnsmateriale til NOU Klimatilpassing., Norsk klimasenter, Oslo, Norway. Klima i Norge 2100 report available: http://www.miljodirektoratet.no/no/Publikasjoner/2015/September-2015/Klima-i-Norge-2100/

Haverd V, Smith B, Nieradzik L, Briggs PR, Woodgate W, Trudinger CM et al (2018) A new version of the CABLE land surface model (Subversion revision r4601) incorporating land use and land cover change, woody vegetation demography, and a novel optimisation-based approach to plant coordination of photosynthesis. Geosci Model Dev 11(7):2995–3026

Hu X, Iordan CM, Cherubini F (2018) Estimating future wood outtakes in the Norwegian forestry sector under the shared socioeconomic pathways. Glob Environ Chang 50:15–24

Mahowald N, Lo F, Zheng Y, Harrison L, Funk C, Lombardozzi D, Goodale C (2016) Projections of leaf area index in earth system models. Earth Syst Dynam 7:211–229. https://doi.org/10.5194/esd-7-211-2016

Majasalmi T, Rautiainen M, Stenberg P, Lukeš P (2013) An assessment of ground reference methods for estimating LAI of boreal forests. Forest Ecol Manag 292:10–18. https://doi.org/10.1016/j.foreco.2012.12.017

Majasalmi T, Eisner S, Astrup R, Fridman J, Bright RM (2017) Enhanced LC-product for Fennoscandia. https://doi.org/10.21350/c9j08bz3. Accessed: 8 Nov 2018

Majasalmi T, Eisner S, Astrup R, Fridman J, Bright RM (2018) An enhanced forest classification scheme for modeling vegetation–climate interactions based on national forest inventory data. Biogeosc. 15:399–412

Naudts K, Ryder J, McGrath MJ, Otto J, Chen Y, Valade A et al (2015) A vertically discretised canopy description for ORCHIDEE (SVN r2290) and the modifications to the energy, water and carbon fluxes. Geosci Model Dev 8:2035–2065

Poulter B, MacBean N, Hartley A, Khlystova I, Arino O, Betts R et al (2015) Plant functional type classification for earth system models: results from the European Space Agency's Land Cover Climate Change Initiative. Geosci Model Dev 8:2315–2328

R Core Team (2017) R: A language and environment for statistical computing. R Foundation for Statistical Computing, Vienna, Austria URL http://www.R-project.org/

Shevliakova E, Pacala SW, Malyshev S, Hurtt GC, Milly PCD, Caspersen JP et al (2009) Carbon cycling under 300 years of land use change: Importance of the secondary vegetation sink. Global Biogeochem Cycles 23(2)

Van Vuuren DP, Carter TR (2014) Climate and socio-economic scenarios for climate change research and assessment: reconciling the new with the old. Clim Chang 122:415–429

Yue C, Ciais P, Luyssaert S, Li W, McGrath MJ, Chang J, Peng S (2018) Representing anthropogenic gross land use change, wood harvest, and forest age dynamics in a global vegetation model ORCHIDEE-MICT v8. 4.2. Geosci Model Dev 11(1):409–428